An Energy Efficient Advanced Comminution Process to Treat Low-Grade Ferrochrome Slag Using High-Pressure Grinding Rolls

Talasetti Santosh [1,2], Chinthapudi Eswaraiah [2], Shivakumar Irappa Angadi [2], Sunil Kumar Tripathy [3,*], Rahul Kumar Soni [2] and Danda Srinivas Rao [2]

[1] Department of Fuel, Minerals and Metallurgical Engineering, Indian Institute of Technology (Indian School of Mines), Dhanbad 826004, India

[2] CSIR-Institute of Minerals and Materials Technology, Bhubaneswar 751013, India

[3] Research and Development Division, Tata Steel Ltd., Jamshedpur 831001, India

* Correspondence: sunilk.tripathy@tatasteel.com or sunilkr.tripathy@gmail.com; Tel.: +91-92040458167

Abstract: The present research aims to analyze the comminution behavior of ferrochrome slag using high-pressure grinding rolls. The laboratory bench scale high-pressure grinding rolls were used to study the three significant variables on the grinding efficiency of ferrochrome slag. The Central Composite Design was used to study the process variables, such as roll gap, applied load, and roller speed. The grinding efficiency was evaluated based on the product size and the energy consumption. The results showed that the increased gap between the rolls and roller speed decreases the product size with increased energy consumption. The results also found that an increase in applied load decreases the product fineness with increased energy consumption. The models were developed for the responses of P_{80} (size of 80% mass finer) and Ecs (specific energy consumption). Both the responses show high regression coefficients, thus ensuring adequate models with the experimental data. The minimum values of the P_{80} size and specific energy were determined using quadratic programming. The optimum values of the roll gap applied load and roll speed were found to be 1.43 mm, 16 kN, and 800 Rpm, respectively. The minimum values of P_{80} and the specific energy consumption were found to be 1264 μm and 0.56 kWh/t, respectively.

Keywords: HPGR; comminution; ferrochrome slag; characterization; energy consumption; product size; modeling

1. Introduction

Day by day, the high-grade ores are depleting, and mineral industries face the low-grade ores and increasing complexity in terms of their mineralogy and fineness of the ore and gangue constituents. The grinding of such low-grade ores/minerals with complex textures is costly and an energy-intensive unit process in the mineral industry [1]. Comminution performs a vital role in most mineral processing plants. It is an energy-intensive unit operation in mineral processing and other processing industries [2]. In a typical mineral processing plant, the comminution circuit alone consumes the most energy [3–6]. High-Pressure Grinding Rolls (HPGR) have begun to be considered for more base metal projects; currently, the rolls surfaces have been developed in such a way as to treat hard and abrasive ores. In 1985, the first HPGR was installed as a primary milling unit in a cement plant. The product obtained from the HPGR directly goes to the milling circuit with a combination of classifiers for efficient separation downstream [7]. The development of high-pressure grinding rolls has been offered as a promising new comminution technology with the benefits of improved grinding efficiency compared to conventional grinding techniques [8].

HPGR is an energy-efficient size-reduction comminution device used in mineral processing industries since the mid-1980s because of its unique ability in energy reduction [9]; improved gangue-mineral value liberation [10]; induction of micro-cracks at the grain-boundaries, which ultimately results in higher grade; and recovery of mineral values in the downstream beneficiation processes [11,12]. The HPGR has been used in the minerals industry, with primary installations in the iron ore pelletizing and diamond industries in the mid-1990s. This technology was used for the different hard rock minerals, i.e., copper, gold, and platinum ore. Recently introduced, HPGRs have high energy and grinding efficiency [8], improved mineral liberation [10], particle weakening [13], and generation when compared with conventional crushers in the mineral industry. High grades and recovery have been reported in the downstream operation due to such changes in material characteristics [11,14–16]. Comminution in HPGR results from the high inter-particle stresses generated when a bed of solid particles is compressed as it moves down the gap between the two pressurized rolls [10,16]. Such high interparticle stresses result in much greater quantities of fines than conventional crushing [11]. HPGRs create a compressive bed of particles between the rolls, utilizing the process of inter-particle breakage, which results in the micro-fracturing of the ore [17]. The confined-bed particle breakage mechanism employed by the HPGR requires less energy to achieve the same degree of size reduction when compared with the conventional crushers [18–20]. In HPGR, the efficiency of comminution depends on several operating variables. Many researchers have studied the influence of operational parameters on HPGR. Saramak and Kleiv [21] have studied the effect of feed moisture on comminution efficiency on the HPGR circuit. Lim et al. [22] investigated the effect of roll speed and rolls surface pattern on HPGR performance. Fuerstenau and Abouzeid [23] studied the role of feed moisture in HPGRs. Therefore, the operating variable performs an important role, and the optimization of variables is crucial for the comminution of the HPGR system.

Ferrochrome slag is generated during the manufacturing of ferrochrome metal, then slag is quenched in water. Generally, these slags are utilized for different applications in ceramic, refractory, and civil constructions [24,25]. However, each application needs a suitable particle size for utilization. The application in civil construction as an aggregate is widely used to utilize slag, and the application requires a certain particle size [26]. During the quenching process, slag is generated at a particle size below 10 mm, and it contains about 1–3% metal. Thus, there is an effort to recover these metals from slag prior to utilizing these as aggregate in civil industry applications. For recovery, the liberation of the metal is necessary, which needs to be grounded prior to separation. Thus, HPGR was applied for the size reduction process to liberate the metals from slag.

The objective of the present research work is to study the influence of operating variables on the performance of HPGR for grinding of ferrochrome slag. The present topic is relevant to the mineral processing field and it describes the energy consumption problem in the size reduction operations to produce finer size material. In the present work, experiments were carried out in a HPGR with ferrochrome slag material. Central Composite Design (CCD) was used to study the process variables, such as a gap between the rolls, applied load, and roller speed. In HPGR, three process variables, such as the gap between the rolls, applied load, and roller speed, have been varied. The regression models have been developed to predict the performance of HPGR. The combined interactional effects of operating variables on process responses were also discussed in detail. The materials and method section in the manuscript discusses the strategy obtaining general information about the ferrochrome slag, such as source of material, material density, sampling procedure, followed by the detailed microscopic characterization of the received ferrochrome slag. The materials and method section also discusses the details of HPGR used to generate experimental data in the present work, and the strategies adopted for development of mathematical models from the generated data. The results and discussion section describes the major outcomes of the work in terms of effect of operating variables on the product size and energy consumption of HPGR operation. Post analysis the effect of various operating

parameters, the section discusses the mathematical representation of such observation followed by the use of such models in optimizing the operating conditions of the HPGR to achieve higher extent of grinding at minimal expense of energy. The conclusion section in the manuscript summarizes the results observed in the present work. The novelty of the present work is to study the ferrochrome material using an energy-efficient advanced comminution technique to prepare the feed material for downstream process to recover more valuable minerals therein.

2. Materials and Methods

2.1. Ferrochrome Slag

Ferrochrome slag from a typical ferrochrome manufacturing unit from Eastern India was used in the present investigation. The density of the slag was found to be 3.1 g/cc. The density of the ore was measured with the help of an air-pycnometer. The material size was reduced to below 10 mm using a jaw crusher to prepare the feed for HPGR experiments. The granulometry of the slag was carried out after being crushed to below 10 mm, and it was found that 80% of the particles were below 6.2 mm (D_{80}). Additionally, the average particle size (D_{50}) of the sample is 3 mm. It is also found that 13.5% of the particles are below 1 mm in size in the slag. The jaw crusher product was subjected to the HPGR comminution. Coning and quartering technique was used to prepare the materials to obtain representative samples for each experimental run. About 20 bags of 10 kg samples were prepared for HPGR tests. The final ground product was sieved based on root two series. The energy consumption was noted down for each experimental condition.

2.2. Characterization Studies

The water quenched ferrochrome slag was analyzed as 8.97% Cr (total) and 2.57% Cr (metal). Optical microscopic studies were carried out on the polished sections of different size fractions of the ferrochrome slag. Wide size ranges of globular and oval-shaped ferrochrome metals within the slag sample were observed and were distributed unevenly (as shown in Figure 1). Reflected light photomicrographs of different sizes classified fractions, as mentioned, is shown in the same figure. Occasionally, the ferrochrome metals contain inclusions of silicates of different shapes and sizes (as shown in Figure 1). The top two photomicrographs shown in Figure 1 indicate that the Fe-Cr metals occurring within the slag are free from any silicate/slag inclusions, but occur within the slag in unliberated conditions. Occasionally, the middle two photographs indicate that the Fe-Cr metals (M) also contain slag inclusions within them. The Fe-Cr slags contain silicate (S) inclusions in various shapes and sizes, including rounded/sphere-shaped (bottom-most right-side photomicrograph). The optical microscopic studies indicated that the ferrochrome slag includes three different types of phases (i) ferrochrome metal, (ii) oxide/non-silicate phases, and (iii) silicate phases. Furthermore, these phases are identified and confirmed through electron microscopes. Additionally, it is found that the liberation size of the chrome bearing phases is finer sizes compared to the free ferrochrome metal. Thus, it is important to liberate those chrome bearing phases prior to separation. It is also confirmed that the liberation of metals in the slag ranges occurs below 2 mm.

2.3. High-Pressure Grinding Rolls

A general configuration of the HPGR involves two counter rotating rollers, known as fixed and floating rolls. The floating roll is pushed towards a fixed roll by the hydraulic pressure created by a piston. The hydraulic press applies pressure for a short time on the material being crushed. The action helps in generating new micro-cracks inside the material, which, in the next step, produce fine particles [27]. The sample was choke-fed to the roll gap, with nip and pre-breakage occurring for particles larger than the gap by single-particle comminution and smaller particles forming a compressed bed between the rolls enabling a more efficient bed breakage mechanics. A HPGR of 1 tph capacity is installed at CSIR-IMMT, Bhubaneswar, shown in Figure 2 was used in the present study. It

has rollers of 200 mm diameter and 100 mm width with adjustable gap between the rollers. The fed particles nipped between the counter rotating rolls are subjected to compressive loads, which perform slow compression of the material. Four load sensors (each 50 kN capacity) measure the load applied by the floating piston and a torque sensor (5000 Nm capacity) fitted at the driving shaft measures the toque applied by the rotating roll along with its rpm of rotation. The power consumption of the machine was measured with the help of an energy meter. The energy consumption on the basis of per unit feed was calculated using the following equation:

$$E_{sp} = \frac{P_t - P_i}{M} \tag{1}$$

where E_{sp} (kWh/t) = net specific energy consumption, P_t (kW) = total main motor power, P_i (kW) = idle main motor power, and M (t/h) = throughput.
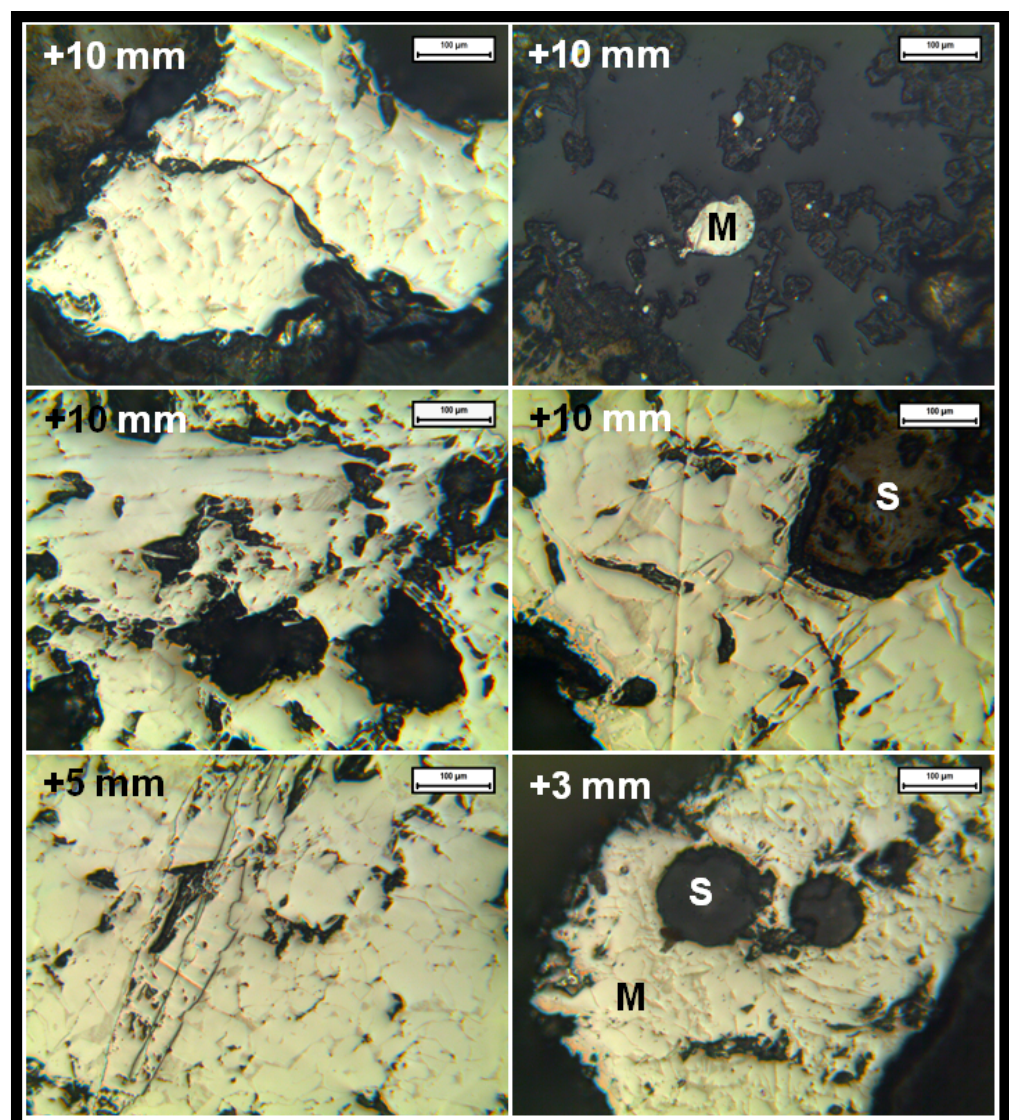

Figure 1. Optical microscopy analysis of particles of ferrochrome slag.

In HPGR, three process variables were varied: the gap between the rolls, applied load, and roller speed. For each experiment, 10 kg of the sample was taken to study the effects of operating parameters. The final ground product was sieved based on the standard series. The energy consumption was noted down for each experimental condition.
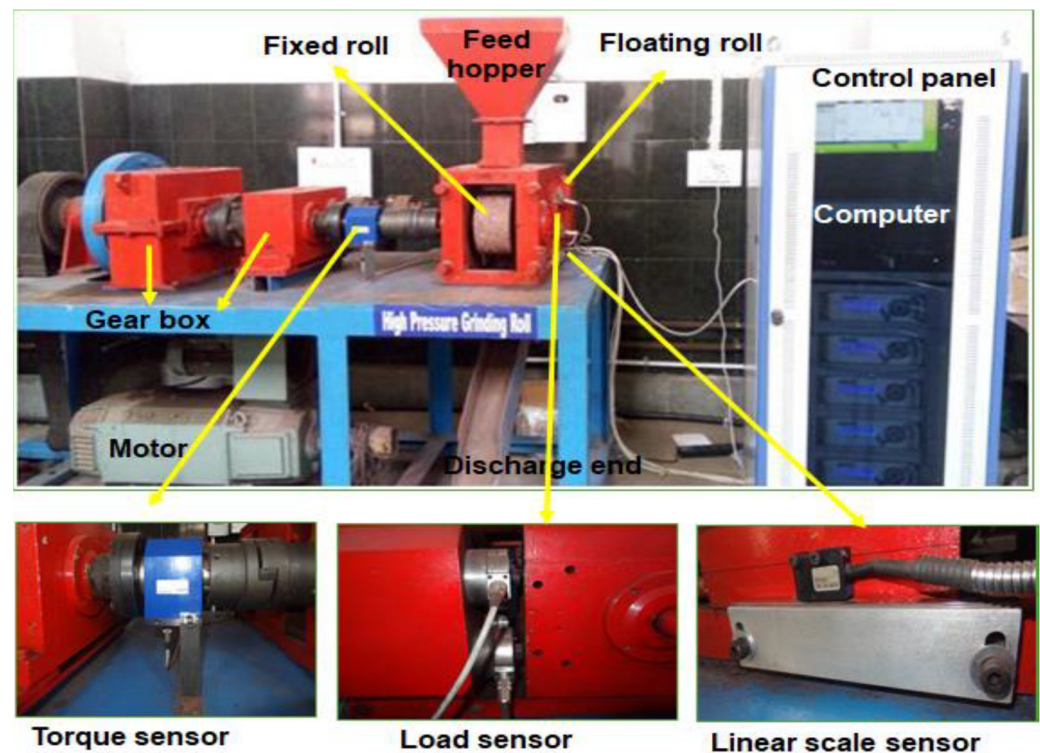
Figure 2. The instrumented laboratory HPGR along with its sensors.

2.4. Response Surface Methodology

Response Surface Methodology (RSM) is one of the methodologies for obtaining the optimum values [28]. For analyzing the process, different process variables, such as the gap between the rolls, applied load, and roller speed, were varied based on the statistically designed experiments. Central composite design along with RSM was considered for the analysis of the findings. Based on the central composite design, a second-order quadratic equation was developed for each response and expressed as mentioned in Equation (2) [29,30]. CCD technique has been widely used as a statistical method involving two or more variables and can develop a nonlinear model for the optimization of process variables. CCD designs have been useful in developing regression based mathematical models, which are further helpful in optimizing the process parameters. This design of experiment approach not only assesses the effect of individual operating parameters on the process outputs, but also investigates the interaction effect between the operating parameters. The CCD has been applied over the past for fitting a second-order model for process optimization and requires only a minimum number of test runs for experimental study. In CCD, each numeric factor is varied over five levels: plus, and minus alpha (axial points, star points), plus and minus 1 (factorial points, corner points of the cube), and the center point.

The design of experiment recommends 20 experiments in total for five-level three-factorial CCD design. Assuming the independent variables are continuous and controllable, one of the objectives of such analysis is to develop models that can predict the dependent output (y) as function of independent parameters (x). The interaction effects between the independent parameters are often represented by response surface methodology (RSM) of second-order models. By using these prediction models, 3D surface plots were processed to predict the interaction of variables for different responses. The experimental results were analyzed through Design Expert software (10.0.8) to develop the prediction models along

with analysis of variance (ANOVA) to evaluate the robustness. Furthermore, the models were used to derive 3D surface plots from the same software.

$$Y = \beta_0 + \sum_{i=1}^{k} \beta_i x_i + \sum_{i=1}^{k} \beta_{ii} x_i^2 + \sum_{i=1}^{k} \sum_{j=1}^{k} \beta_{ij} x_{ij} x_{ji} + \varepsilon \tag{2}$$

The total number of patterns of a particular type of order is given by k. β_i, β_{ij}, and β_{ii} in the model represents coefficients for the linear, interaction, and quadratic terms, respectively. B_0 and ε in the model represents final adjustment coefficient and final error term, respectively. The independent parameters (x_i) are the coded form of the parameter obtained with the help of actual/uncoded values (X_i) of the parameters and central value of actual/uncoded parameter as:

$$x_i = (X_i - X_0) / \Delta X_i \tag{3}$$

In the present investigation, a central composite design (CCD) matrix was chosen to study the effect of operating variables on the performance of HPGR. In this study, 20 sets of experiments with appropriate combinations of the gap between the rolls (x_1), applied load (x_2), and roller speed (x_3) were discussed in detail. The range and levels of the operating variables are presented in Table 1.

Table 1. Actual and coded values of the operating variables.

Independent Variables	Symbol		Coded Levels		
	Un-Coded	Coded	−1	0	+1
Roll gap, mm	x_1	X_1	0.8	1.2	1.6
Applied load, kN	x_2	X_2	8	12	16
Roller speed, Rpm	x_3	X_3	500	650	800

3. Results and Discussion

### 3.1. Grinding Studies Using HPGR

The CCD matrix was used for the design of HPGR experiments for ferrochrome slag. The effect of three significant operating variables, namely, roll gap, applied load, and roller speed was studied. The operating variables range, and levels are given in Table 1. The process responses, i.e., energy consumption and product size, are considered in the present study. A total of 20 experiments were conducted, out of which, six experiments were performed at the base level for estimation of the experimental error. The grinding experiments were performed at five levels, i.e., low level (−2), +1, middle level (0), −1, and high level (+2) (Table 1). The actual and coded factor values and the respective values of responses for all the experiments are given in Table 2. The experimental results were analyzed through Design Expert software (10.0.8). Mathematical models were developed for both the responses based on the theoretical background discussed in Section 2.4. The predicted values of the response of product size and energy consumption were obtained from the quadratic model equations using the Design-Expert 10 version 10.0.8. The interactional effects of operating variables were discussed in the form of 3D response surface plots, which were constructed using predicted second order quadratic equations. The description of the approach adopted for obtaining the response surface plots along with theoretical basis associated with it can be referred from Section 2.4.

Table 2. Central composite design of independent variables expressed in coded and actual levels with responses.

Run No	Coded Levels			Gap, mm	Load, kN	Roller Speed, Rpm	Energy, kWh/t	P_{80}, µm
1	0	0	−1.68	1.2	12	400	0.5	1445
2	0	+1.68	0	1.2	18.7	650	0.63	1345
3	0	−1.68	0	1.2	5.3	650	0.53	1407
4	0	0	0	1.2	12	650	0.57	1376
5	−1.68	0	0	0.5	12	650	0.53	1395
6	+1	+1	+1	1.6	16	800	0.59	1249
7	+1.68	0	0	1.9	12	650	0.69	1358
8	0	0	0	1.2	12	650	0.55	1380
9	−1	+1	−1	0.8	16	500	0.64	1384
10	0	0	0	1.2	12	650	0.59	1370
11	0	0	0	1.2	12	650	0.53	1382
12	+1	+1	−1	1.6	16	500	0.62	1473
13	0	0	0	1.2	12	650	0.56	1375
14	0	0	0	1.2	12	650	0.57	1377
15	+1	−1	+1	1.6	8	800	0.66	1314
16	−1	−1	−1	0.8	8	500	0.72	1394
17	0	0	+1.68	1.2	12	900	0.54	1305
18	−1	−1	+1	0.8	8	800	0.79	1447
19	−1	+1	+1	0.8	16	800	0.66	1325
20	+1	−1	−1	1.6	8	500	0.61	1425

3.2. Characterization of HPGR Product

Characterization studies indicate that the ferrochrome slag sample contains different shapes and sizes of slag as well as metal phases that are highly heterogeneous. Hence, the slag-metal matrix behaves significantly different when subjected to grinding. The various phases in the slag sample consist of six major elements (Si, Al, Mg, Cr, and Fe) with traces of Na, K, Ca, Ti, Mn, Ni, P, and S [25]. It is also confirming that the metal phases are of different and complex compositions. They indicated that the metal and complex phase have a wide range of density and specific gravity, behaving differently during the normal grinding process. To better understand the breakage mechanism, some of the particles, after crushing, are studied under a microscope, and the findings are shown in Figure 3. In general, textural characteristics perform a vital role in comminution of particle. The energy required to break a particle is governed by the hardness of ore and textural patterns of the crystals. Thus, to create a crack/micro-crack along the grain boundaries, HPGR is a unique comminution unit which has merits to use in the comminution flowsheet. Thus, it is very important to analyze the textural aspects of the crushed product to envisage the features. From Figure 3a–d is the screened products (+5 mm) after grinding, while (e and f) are +3 mm size classified fractions of experiment number 1 with pressure 12 kN. A single crack crossing across a Fe-Cr metal is also found, as shown in Figure 3a,d,e. Similarly, it is also observed that two cracks are crossing a slag phase containing rounded Fe-Cr metals and, as shown in Figure 3b,c,f, the thickness of the cracks varies based on the phases of the particle and the process conditions applied. Thus, with these cracks and micro-cracks, the energy required for the fine grinding can be minimized with better liberation aspects, which is not included in the present study. Hence, HPGR grinding may be a better solution than the normal grinding process [13,31].
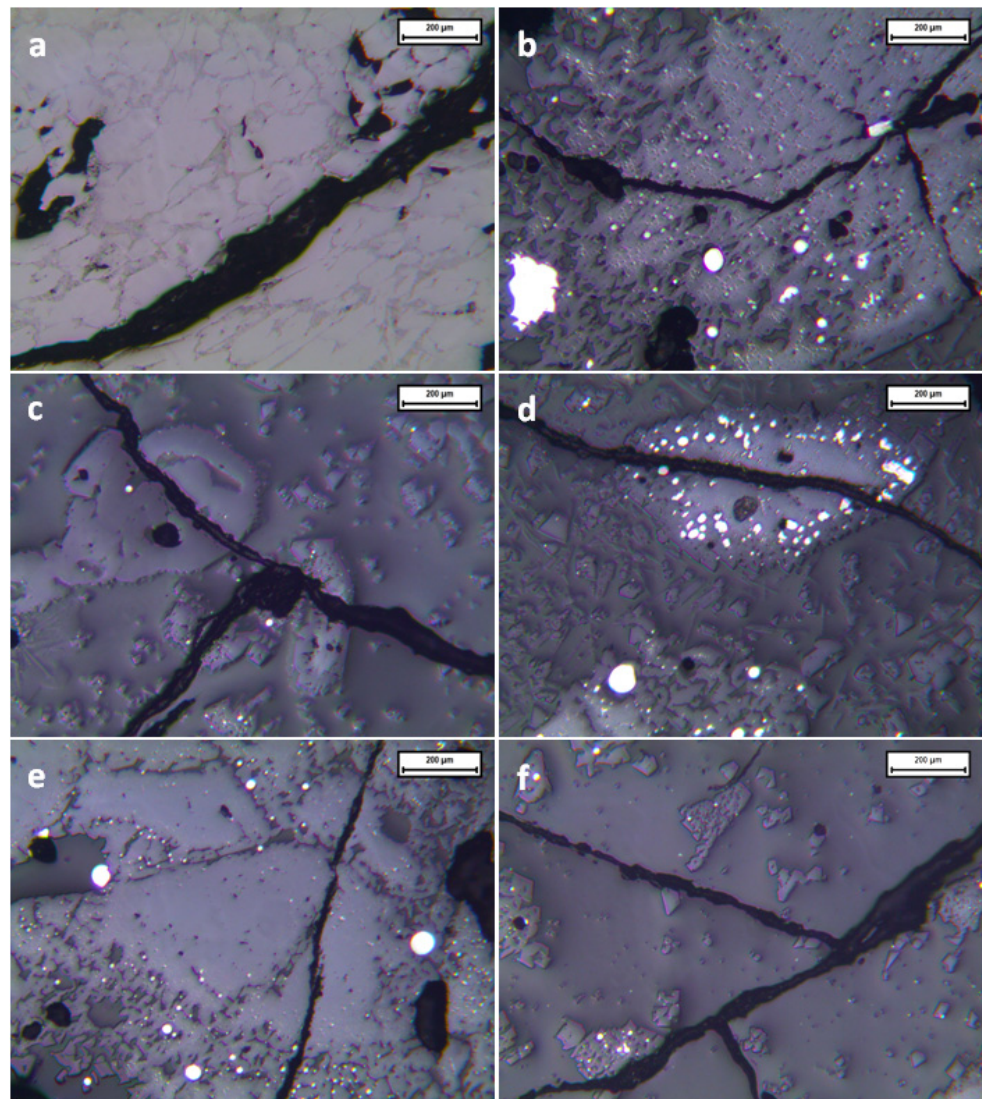
Figure 3. Micrographs of the grounded products after HPGR (coarser sized fractions of +5 and +3 mm).

3.3. Effect of Operating Variables

3.3.1. Rolls Gap

An optimum value of the roll gap is critical in determining the nipping of feed particles, and, therefore, throughput. In certain scenarios, even the particles bigger than roll gap do not slip between the rolls. The slipping between the particles and rolls causes blockage of feed, unsteady operation, and excessive localized stress on the roll surface. The roll gap of HPGR in the present work was varied from 0.5 mm to 1.9 mm to study the effect of the gap between the rolls on the product size and energy consumption. The effect of the roll gap on energy consumption and product size are shown in Figure 4. Three data points were obtained based on the run number 4, 5, 7, 8, 10, 11, 13, and 14 (Table 2). The outcomes of experiments with common operating conditions were averaged for better statistical reliability. As shown in Figure 4, the increase in rolls gap decreases the product size and increases energy consumption. However, the correlation is contradicting to the theory and may be reported due to minimum experimentation as per the DOE. Among all the experiments, the smallest 80% passing size of the product, 1358 µm, was noticed at an energy consumption of 0.69 kWh/t at the lowest rolls gap of 1.9 mm. It was observed that with the increase in roll gap from 0.5 mm to 1.9 mm, the product size became finer. The finer product size was observed at a higher roll gap. The obscure correlation observed

needs further experimentation and analysis along with proper understanding of the role of nip angle and pressure along with their interactional influence.
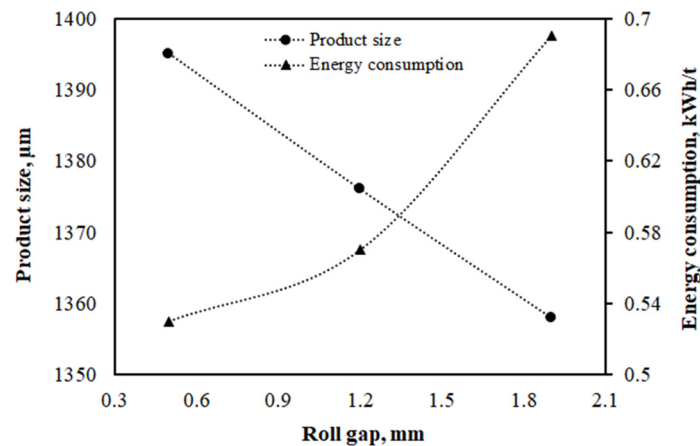
Figure 4. Effect of the gap between the rolls on product size and energy consumption at 12 kN applied load and 650 Rpm roller speed.
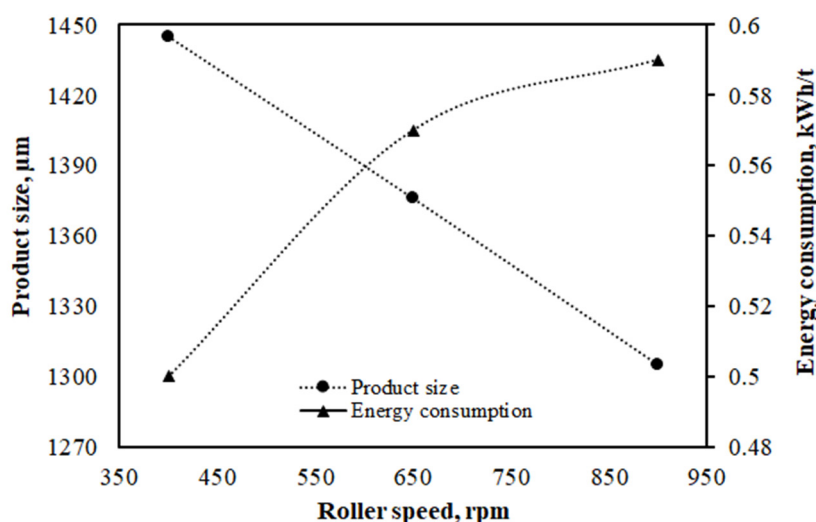
3.3.2. Effect of Applied Load

The applied grinding load is expressed in terms of specific pressing force. Determining the optimum pressing force is an important consideration since it varies with ore characteristics. The energy consumption in HPGR also depends on the applied load. In this study, the range of applied load varied from 5 kN to 19 kN. The effect of applied load on product size and the energy consumption is shown in Figure 5. It was observed that an increase in applied load from 5 kN to 19 kN decreases product size from 1407 μm to 1345 μm. An increase in applied load increases the energy consumption from 0.53 kWh/t to 0.63 kWh/t. From Figure 5, a linear trend was observed for both the product size and energy consumption. With an increase in the specific force, there is a rise in the torque of the motor. In other words, at higher torque, there will be more specific power requirement to crush the particles. It is also found that the trends in the product size distribution and energy drawn are opposite to each other. It can be suggested that the HPGR should be operated with an optimum applied load for better grinding results.
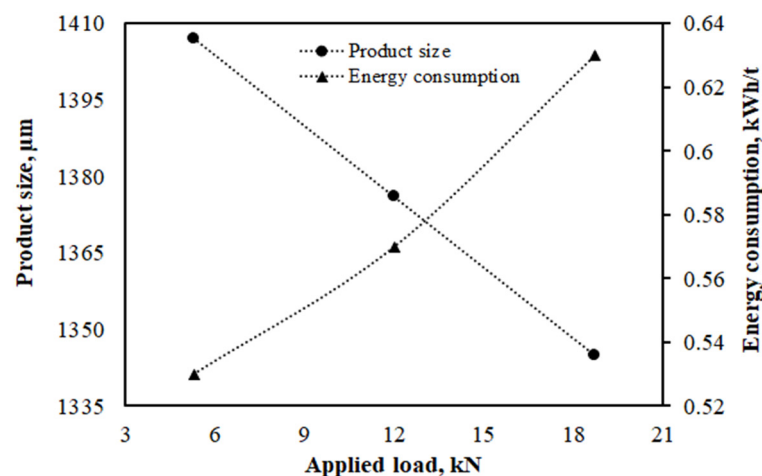
Figure 5. Effect of applied load on product size and energy consumption at 1.2 mm gap and 650 rpm roller speed.

3.3.3. Effect of Roller Speed

Roller speed is an essential operating parameter in the HPGR system. The energy efficiency of comminution increases with increasing rolls speed. In the present work, the rolls speed was varied from 400 Rpm to 900 Rpm to study the effect on product size and energy consumption, as shown in Figure 6. The data points for the plot were obtained in a similar averaging manner that of Section 3.3.1. It was observed that an increase in rolls speed decreases the product size (1445 to 1305 μm) and increases energy consumption (0.5 kWh/t to 0.59 kWh/t). Ref. [17] studied the effect of rolls speed on a range of ore types and machine scales over a wider range of speeds from 0.38 m/s up to 3.1 m/s. The test results stated that the higher roller speed led to finer products for gold and iron ore. An increase in roller speed caused lower proportions of fine and coarse particles to be produced for bauxite and iron ore. It was found that the rolls speed has a significant effect on the grinding efficiency in HPGR. In other words, at higher roll speed, there is an increase in the throughput. This can be explained with lower retention time experienced by the particle at nipping and crushing zone of HPGR at higher roller speed. Thus, it is always advised to operate the HPGR at a higher roll speed to achieve a higher reduction ratio, along with the higher throughput. From the experimental study, it was observed that the finer product size was obtained at a higher roller speed.

Figure 6. Effect of roller speed on product size and energy consumption at 1.2 mm gap and 12 kN applied load.

3.4. Modeling and Statistical Analysis

Analysis of Variance (ANOVA) is a statistical testing method of the second-order models in the form of linear, squared, and interaction terms used in the present study. From the experimental results in Table 2 and Equation (3), the second-order quadratic response functions representing the energy consumption and product size could be expressed as functions of the gap, applied load, and roller speed. The results were analyzed using the Design expert 10.0.8 software package, and model fitting was carried out to identify the appropriate models for the response variable. It was found that quadratic models fit well for both energy consumption and product size. To represent the significance of the individual, interaction, and square effects in the models, the probability values (*p*-values) were considered. To predict the product size and energy consumption, the quadratic model was found to be highly significant and appropriate compared to other models, accounting for more than 98% and 99% variations in the observed data, respectively. The model was developed using these factors and their interaction presented in Equations (4) and (5).

$$Y_1 = 1.31 - 1.2X_1 - 0.06X_2 + 0.0014X_3 + 0.01X_1X_2 - 0.000145X_1X_3 - 0.000027X_2X_3 + 0.44X_1^2 + 0.0026X_2^2 \atop -0.00000063X_3^2 \tag{4}$$

$$Y_2 = 864.57 + 310.7X_1 + 15.38X_2 + 1.13X_3 + 8.98X_1X_2 - 0.68X_1X_3 - 0.04X_2X_3 - 0.29X_1^2 - 0.014X_2^2 \atop -0.000025X_3^2 \tag{5}$$

where Y_1 and Y_2 are the process responses (energy consumption expressed in kWh/t and product size expressed in μm, respectively) and X_1, X_2, and X_3 are the gap (mm), applied load (kN), and roller speed (Rpm), respectively.

The ANOVA for the product size and energy consumption are given in Table 3. The F-value of energy consumption and product size was 70.26 and 653.19, respectively. The *p*-values less than 0.05 signify the rejection of the null hypothesis at a 95% confidence level, which indicates a particular term in the model significantly affects the response. Therefore, the *p*-value for both models was acceptable, which indicated the developed models were significant. The interaction effects of operating variables are presented in 3D response surface plots on the process responses.

Table 3. Analysis of variance for the energy consumption and product size.

Statistics	Energy Consumption, kWh/t	Product Size, μm
Sum of squares	0.14	52,219
Degree of freedom	9	9
Mean sum of square	0.016	5802
F-value	70.26	653.19
Prob > F	<0.0001	<0.0001
R^2	0.98	0.99
Adj. R^2	0.97	0.99

All the main effects, linear, square, and interactions, were computed for each model. The predicted energy consumption values obtained from Equation (4) were closely matched with the observed values, implying that the model was pertinent enough. From Equation (4), the coefficient of determination ($R^2 = 0.98$) predicting energy consumption was highly significant. Similarly, from Equation (5), the coefficient of determination ($R^2 = 0.99$) used to predict the product size was highly satisfactory. Furthermore, a high value of adjusted correlation coefficient indicates a strong correlation and dependence between the predicted and observed values of Ecs and P_{80}.

3.5. Three-Dimensional Response Surface Plots

The 3D response surface plots help to understand the main and interaction effects on the responses in a straightforward manner. In this study, the regression models developed have three independent variables: roll gap, applied load, and roller speed. Therefore, based on the quadratic model equations developed for the product size and energy consumption, the effects of the independent variables and their interactions were represented in terms of 3D response surface plots.

3.5.1. Product Size

The interactional effects of gap-load, gap-roller speed and load-roller speed on product size consumption as shown in Figure 7a–c. Figure 7a shows the interactional effect of the gap between the roll and applied load on product size. It was observed that the increase in roll gap and applied load decreases the product size. Finer product size was obtained at a higher level of roll gap and applied load. It was also observed that the roll gap has a predominant effect on product size compared to the applied load. The interactional effect of rolls gap and roller speed is shown in Figure 7b. It was observed from the decrease in

roll gap produces finer size material in Figure 7b. In the case of roller speed, an increase in roller speed decreases the product size. The finer product size was obtained at a lower level of roll gap and a higher level of roller speed. Similarly, the interactional effect of applied load and roller speed is plotted and shown in Figure 7c. An increase in applied load and roller speed decreases the product size drastically. Abazarpoor et al. [28] studied the effect of three operating variables on d_{80} and Blaine using response surface methodology. It was found that the roller speed and specific pressure significantly affects the fineness (d80). Feed moisture had little influence on the process responses. It was observed from present study, finer product size obtained at a higher level of applied load and roller speed. Roller speed had more impact on the product size as compared to the applied load.
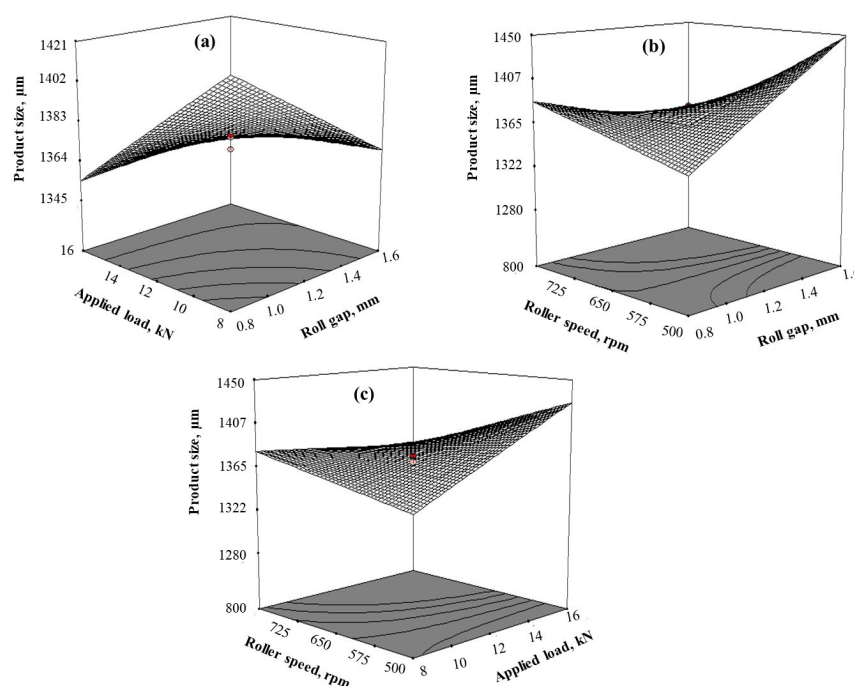
Figure 7. (**a**–**c**). Response surface plots showing the interactional effects of (**a**) roll gap-applied load, (**b**) roll gap-roller speed, and (**c**) applied load-roller speed for product size.

3.5.2. Energy Consumption

The interactional effects of gap-load, gap-roller speed, and load-roller speed on energy consumption, as shown in Figure 8a–c. Figure 8a shows the interactional effect of the gap between the rolls and applied load on energy consumption. In HPGR, the grinding efficiency mainly depends on the operating rolls gap. It operates with two counter-rotating rolls; HPGR creates a compressive bed of particles between the rolls, utilizing the inter-particle comminution mechanism. It was observed that the lowest energy consumption was obtained at a lower level of the gap between the rolls and applied load. The interactional effect of the gap between the rolls and roller speed on energy consumption is plotted, as shown in Figure 8b. Rolls gap and roller speed are important operating variables in HPGR, which directly influences the process responses. An increase in rolls gap and roller speed increases energy consumption. It was observed that the lowest energy consumption was obtained at a lower level of roller gap and roller speed. Similarly, the interactional effect of applied load and roller speed on energy consumption is shown in Figure 8c. After the increase in applied load, there is a marginal increase in energy consumption. Roller speed increases with an increase in energy consumption. It was observed that the lowest energy consumption was obtained at a lower level of applied load and a higher level of roller speed.
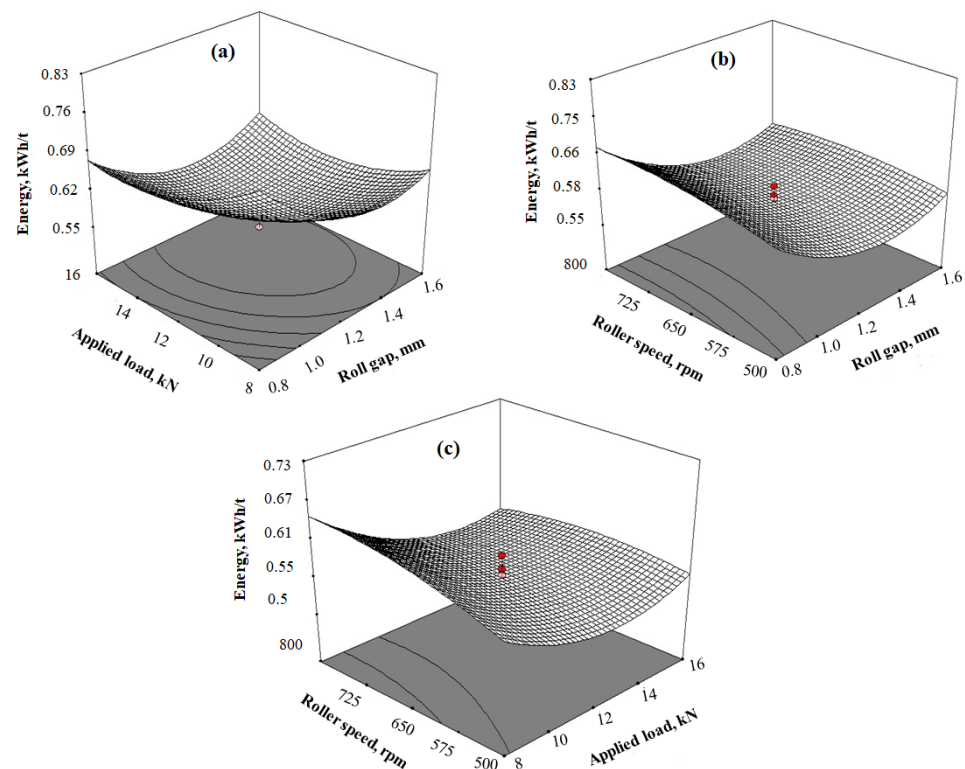
Figure 8. Response surface plots showing the interactional effects of (**a**) gap-applied load, (**b**) gap-roller speed, and (**c**) applied load-roller speed for energy consumption.

3.6. Optimization Studies

The HPGR is an important advanced comminution technique to reduce energy consumption in slag applications. The model equations developed were optimized using quadratic programming of the mathematical software package (Design Expert 10.0.8) to obtain a target product size within the experimental range investigated. The improvement of grinding performance was verified at the optimal levels of factors selected. Optimization of the process is an important aspect which can be used to visualize the optimum energy required to generate the finer particle size in the crushed product of HPGR. The optimization was targeted to achieve a finer product size with minimum energy consumption. Six more additional grinding tests were conducted at optimal conditions to validate the predictive capability of the models developed. The optimum levels of variables were found to be a 1.43 mm gap, 16 kN applied load, and 800 Rpm roller speed. The optimization results were found to be 0.56 kWh/t energy consumption and 1264 μm product size. The validated tests were found to be accurate with an error of +5%. However, the optimization findings are material specific and may not be valid for other material due to different grinding/crushing characteristics.

4. Conclusions

The HPGR technology is currently one of the most efficient methods for hard ore comminution. Comminution experiments were conducted in a laboratory HPGR for ferrochrome slag material. This study investigated the effect of operating variables, i.e., rolls gap, applied load and roller speed, on the grinding of a ferrochrome slag. The grinding efficiency of HPGR is evaluated based on the product size and the energy consumption. The test results stated that the operating variables have a significant effect on the product size and energy consumption. The HPGR test concluded that rolls gap, applied load, and roller speed were statistically significant on product size and energy consumption. A quadratic model with a coefficient of determination (R^2) of 0.99 and 0.98 was derived for the product size and energy consumption. Response surface methodology was applied to

identify the optimal conditions. The operating variables and responses were optimized. The optimized results were found to be a 1.43 mm gap, 16 kN load, and 800 Rpm roller speed. The responses were found to be 0.56 kWh/t energy consumption and 1264 μm product size. The obtained test results were useful to the milling process for further size reduction to prepare feed material for downstream beneficiation process. It was concluded that HPGR is an energy-saving advanced comminution technique to treat ferrochrome slag material.

Author Contributions: Conceptualization, C.E., S.I.A. and S.K.T.; methodology, C.E., S.I.A. and S.K.T.; software, C.E., T.S. and R.K.S.; validation, C.E., T.S. and R.K.S.; formal analysis, C.E. and T.S.; investigation, C.E., T.S. and D.S.R.; resources, C.E., S.I.A. and S.K.T.; data curation, C.E. and T.S.; writing—original draft preparation, T.S., C.E. and S.K.T.; writing—review and editing, T.S., C.E., D.S.R. and S.K.T.; visualization, C.E., S.K.T., S.I.A. and D.S.R.; supervision, C.E. and S.K.T.; project administration, S.I.A. and S.K.T.; funding acquisition, S.I.A. and S.K.T. All authors have read and agreed to the published version of the manuscript.

Conflicts of Interest: The authors declare no conflict of interest.

References

1. Santosh, T.; Soni, R.K.; Eswaraiah, C.; Rao, D.S.; Venugopal, R.; Kumar, S. Modeling and application of stirred mill for coarse grinding of PGE bearing chromite ore. *Sep. Sci. Technol.* **2023**, *58*, 2075754. [CrossRef]
2. Saeidi, N.; Noaparast, M.; Azizi, D.; Aslani, S.; Ramadi, A. A Developed Approach Based on Grinding Time to Determine Ore Comminution Properties. *J. Min. Environ.* **2013**, *4*, 105–112. [CrossRef]
3. Fuerstenau, D.W.; Kapur, P.C.; Gutsche, O. Comminution of Single Particles in a Rigidly-Mounted Roll Mill Part 1: Mill Torque Model and Energy Investment. *Powder Technol.* **1993**, *76*, 253–262. [CrossRef]
4. Meghwal, M.; Goswami, T.K. Evaluation of Size Reduction and Power Requirement in Ambient and Cryogenically Ground Fenugreek Powder. *Adv. Powder Technol.* **2013**, *24*, 427–435. [CrossRef]
5. Choi, H.; Lee, W.; Kim, S. Effect of Grinding Aids on the Kinetics of Fine Grinding Energy Consumed of Calcite Powders by a Stirred Ball Mill. *Adv. Powder Technol.* **2009**, *20*, 350–354. [CrossRef]
6. Kotake, N.; Suzuki, K.; Asahi, S.; Kanda, Y. Experimental Study on the Grinding Rate Constant of Solid Materials in a Ball Mill. *Powder Technol.* **2002**, *122*, 101–108. [CrossRef]
7. Sesemann, Y.; Broeckmann, C.; Höfter, A. A New Laboratory Test for the Estimation of Wear in High Pressure Grinding Rolls. *Wear* **2013**, *302*, 1088–1097. [CrossRef]
8. Ozcan, O.; Aydogan, N.A.; Benzer, H. Effect of Operational Parameters and Recycling Load on the High Pressure Grinding Rolls (HPGR) Performance. *Int. J. Miner. Process.* **2015**, *136*, 20–25. [CrossRef]
9. Schönert, K. A First Survey of Grinding with High-Compression Roller Mills. *Int. J. Miner. Process.* **1988**, *22*, 401–412. [CrossRef]
10. Kodali, P.; Dhawan, N.; Depci, T.; Lin, C.L.; Miller, J.D. Particle Damage and Exposure Analysis in HPGR Crushing of Selected Copper Ores for Column Leaching. *Miner. Eng.* **2011**, *24*, 1478–1487. [CrossRef]
11. Tavares, L.M. Particle Weakening in High-Pressure Roll Grinding. *Miner. Eng.* **2005**, *18*, 651–657. [CrossRef]
12. Yin, W.; Chen, K. Effect of the Particle Size and Microstructure Characteristics of the Sample from HPGR on Column Bioleaching of Agglomerated Copper Ore. *Hydrometallurgy* **2021**, *200*, 105563. [CrossRef]
13. Aminalroaya, A.; Pourghahramani, P. Investigation of Particles Breakage and Weakening Behaviors in Multi-Component Feed Grinding by High Pressure Grinding Rolls (HPGR). *Miner. Process. Extr. Metall. Rev.* **2021**, *43*, 217–232. [CrossRef]
14. Saramak, D.; Wasilewski, S.; Saramak, A. Influence of copper ore comminution in HPGR on downstream minerallurgical processes. *Arch. Metall. Mater.* **2017**, *62*, 1689–1694. [CrossRef]
15. Van Der Meer, F.P.; Maphosa, W. High pressure grinding moving ahead in copper, iron, and gold processing. *J. S. Afr. Inst. Min. Metall.* **2012**, *112*, 637–647.
16. Liu, L.; Tan, Q.; Liu, L.; Cao, J. Comparison of Different Comminution Flowsheets in Terms of Minerals Liberation and Separation Properties. *Miner. Eng.* **2018**, *125*, 26–33. [CrossRef]
17. Yin, W.; Tang, Y.; Ma, Y.; Zuo, W.; Yao, J. Comparison of Sample Properties and Leaching Characteristics of Gold Ore from Jaw Crusher and HPGR. *Miner. Eng.* **2017**, *111*, 140–147. [CrossRef]
18. Ballantyne, G.R.; Hilden, M.; van der Meer, F.P. Improved Characterisation of Ball Milling Energy Requirements for HPGR Products. *Miner. Eng.* **2018**, *116*, 72–81. [CrossRef]
19. Fuerstenau, D.W.; Shukla, A.; Kapur, P.C. Energy Consumption and Product Size Distributions in Choke-Fed, High-Compression Roll Mills. *Int. J. Miner. Process.* **1991**, *32*, 59–79. [CrossRef]

20. Fuerstenau, D.W.; Lutch, J.J.; De, A. The Effect of Ball Size on the Energy Efficiency of Hybrid High-Pressure Roll Mill/Ball Mill Grinding. *Powder Technol.* **1999**, *105*, 199–204. [CrossRef]

21. Saramak, D.; Kleiv, R.A. The Effect of Feed Moisture on the Comminution Efficiency of HPGR Circuits. *Miner. Eng.* **2013**, *43–44*, 105–111. [CrossRef]

22. Lim, W.I.L.; Campbell, J.J.; Tondo, L.A. The Effect of Rolls Speed and Rolls Surface on High Pressure Grinding Rolls Performance. *Miner. Eng.* **1997**, *10*, 401–419. [CrossRef]

23. Fuerstenau, D.W.; Abouzeid, A.Z.M. Role of Feed Moisture in High-Pressure Roll Mill Comminution. *Int. J. Miner. Process.* **2007**, *82*, 203–210. [CrossRef]

24. Sahu, N.; Biswas, A.; Kapure, G.U. A Short Review on Utilization of Ferrochromium Slag. *Miner. Process. Extr. Metall. Rev.* **2016**, *37*, 211–219. [CrossRef]

25. Sahu, N.; Biswas, A.; Kapure, G.U. Development of Refractory Material from Water Quenched Granulated Ferrochromium Slag. *Miner. Process. Extr. Metall. Rev.* **2016**, *37*, 255–263. [CrossRef]

26. Patla, S.; Mondal, S.; Choudhary, A.K. On Improving the Performance of Silty Soil by Treating with Ferrochrome Slag: An Experimental Study. In Proceedings of the Indian Geotechnical Conference 2019, Surat, India, 19–21 December 2019; Springer: Singapore, 2021; pp. 325–335.

27. Torres, M.; Casali, A. A Novel Approach for the Modelling of High-Pressure Grinding Rolls. *Miner. Eng.* **2009**, *22*, 1137–1146. [CrossRef]

28. Abazarpoor, A.; Halali, M.; Hejazi, R.; Saghaeian, M. HPGR Effect on the Particle Size and Shape of Iron Ore Pellet Feed Using Response Surface Methodology. *Miner. Process. Extr. Metall. Trans. Inst. Min. Metall.* **2018**, *127*, 40–48. [CrossRef]

29. Kwak, J.S. Application of Taguchi and Response Surface Methodologies for Geometric Error in Surface Grinding Process. *Int. J. Mach. Tools Manuf.* **2005**, *45*, 327–334. [CrossRef]

30. Aslan, N. Application of Response Surface Methodology and Central Composite Rotatable Design for Modeling and Optimization of a Multi-Gravity Separator for Chromite Concentration. *Powder Technol.* **2008**, *185*, 80–86. [CrossRef]

31. Aminalroaya, A.; Pourghahramani, P. The Effect of Feed Characteristics on Particles Breakage and Weakening Behavior in High Pressure Grinding Rolls (HPGR). *Miner. Process. Extr. Metall. Rev.* **2021**, *43*, 610–621. [CrossRef]